Constructing an Axonal-Specific Myelin Developmental Graph and its Application to Childhood Absence Epilepsy

Gerhard S. Drenthen, Eric L. A. Fonseca Wald, Walter H. Backes, Albert P. Aldenkamp, R. Jeroen Vermeulen, Mariette H. J. A. Debeij-van Hall, Sylvia Klinkenberg, Jacobus F. A. Jansen

From the School for Mental Health and Neuroscience, Maastricht University Medical Center, P. Debyelaan 25, Maastricht, The Netherlands (GSD, ELAFW, WHB, APA, RJV, SK, JFAJ); Department of Radiology and Nuclear Medicine, Maastricht University Medical Center, P. Debyelaan 25, Maastricht, The Netherlands (GSD, WHB, JFAJ); Department of Electrical Engineering, Eindhoven University of Technology, De Rondom 70, Eindhoven, The Netherlands (GSD, APA, JFAJ); Department of Neurology, Maastricht University Medical Center, P. Debyelaan 25, Maastricht, The Netherlands (ELAFW, RJV, SK); and Department of Behavioral Sciences, Epilepsy Center Kempenhaeghe, Sterkselseweg 65, Heeze, The Netherlands (ELAFW, APA, MHJADH).

ABSTRACT

BACKGROUND AND PURPOSE: **The process of myelination starts in utero around 20 weeks of gestation and continues through adulthood. We first set out to characterize the maturation of the tract-specific myelin content in healthy subjects from childhood (7-12 years) into adulthood (18-32 years). Second, we apply the resulting development graph to children with childhood absence epilepsy (CAE), a pediatric epilepsy that was previously characterized by changes in myelin content.**

METHODS: **In a prospective cross-sectional study, 15 healthy children (7-12 years), 14 healthy adult participants (18-32 years) and 17 children with a clinical diagnosis of CAE (6-12 years) were included. For each participant, diffusion weighted images were acquired to reconstruct bundles of white matter tracts and multi-echo multi-slice GRASE images were acquired for myelin-water estimation. Subsequently, a tract-specific myelin development graph was constructed using the percentual difference in myelin-water content from childhood (12 year) to adulthood (25 year).**

RESULTS: **The graph revealed myelination patterns, where tracts in the central regions myelinate prior to peripheral tracts and intra-hemispheric tracts as well as tracts in the left hemisphere myelinate prior to inter-hemispheric tracts and tracts in the right hemisphere, respectively. No significant differences were found in myelin-water content between children with CAE and healthy children for neither the early developing tracts, nor the tracts that develop in a later stage. However, the difference between the myelin-water of late and early developing tracts is significantly smaller in the children with CAE.**

CONCLUSION: **These results indicate that CAE is associated with widespread neurodevelopmental myelin differences.**

Keywords: Maturation, white matter, diffusion MRI, tractography, myelin-water.

Acceptance: Received February 19, 2020, and in revised form March 18, 2020. Accepted for publication March 20, 2020.

Correspondence: Address correspondence to Dr. J.F.A. Jansen, Ph.D., Department of Radiology and Nuclear Medicine, Maastricht University Medical Center, PO Box 5800, 6202 AZ Maastricht, The Netherlands. E-mail: jacobus.jansen@mumc.nl

Acknowledgement and Disclosure: This research did not receive any specific grant from funding agencies in the public, commercial, or not-for-profit sectors.

J Neuroimaging 2020;30:308-314.
DOI: 10.1111/jon.12707

Introduction

Human brain development is a complex process that starts in the third gestational week and continues into adulthood. An important structural component for healthy neuronal maturation of the white matter is the myelin sheath. The myelin sheath is an electrically insulating material that is wrapped around the axons allowing fast and efficient conduction of electrical signals in the central nervous system. The process of myelination is most active during the first 2 years of life, but continues well through adulthood.[1,2] During healthy development, myelin develops in specific patterns related to neurodevelopmental milestones,[3,4] generally proceeding from inward to outward regions, and in the posterior to anterior direction.[5] Abnormalities in the myelin content are associated with several neurological and neuropsychiatric disorders such as Alzheimer's disease, multiple sclerosis, epilepsy, Parkinson's disease, and schizophrenia.[6–11]

The organization of the human brain can be regarded as a complex network, where local clusters of neurons (grey matter) are interconnected via long-range axons (white matter). Bundles of axons in the white matter can be reconstructed using diffusion tensor imaging (DTI), which enables the characterization of the structural brain network in terms of white matter tracts that interconnect remote grey matter regions. Previously, tract-specific increases of Fractional Anisotropy (FA) were reported during childhood and adolescence.[12] FA is often used as a marker of myelin content, however, it is not specific for myelin. For example, while the myelin content does indeed affect the FA to some extent, it is also driven by the density and diameter of axons, fiber orientations and changes to membrane permeability.[13] Moreover, the radial diffusivity (RD) was previously found to reduce during childhood and adolescence.[14] The RD has been demonstrated to be inversely related to the myelin content;[15] however, the RD is also not specific to the

myelin content and is confounded by aspecific changes in water content.[16]

Water is an important component of the myelin, making up to 40% of the total myelin volume. Therefore, myelin-water imaging (MWI) has been extensively applied to estimate the in vivo myelin content. Due to motion restrictions at the microscopic level, the T2 signal arising from water that is trapped between the myelin sheath decays more quickly compared to more freely moving water in the intra- and extracellular spaces. Using T2 relaxometry and multi-exponential analysis the different water components can be decomposed from the total signal, and the myelin-water fraction can be obtained as the fraction of myelin-water signal over the total signal (ie, MWF).[17]

Combining the structural information from DTI with information on the myelin content from MWI might provide a more comprehensive description of the white matter organization in the brain, compared to only the DTI-derived tract trajectories. Previously, it was already shown that myelin-water maps possess distinct patterns along DTI-derived tracts.[18,19] Ideally, it should be feasible to follow the myelin development of various white matter tracts over time, and differentiate tracts that reflect abnormalities during healthy development. While neurological disorders such as multiple sclerosis show severe disruption of the myelin content, other more subtle and developmental changes might play a role in pediatric epilepsies at various time-points of development. For example, a lower frontal myelin content was reported in children with childhood absence epilepsy (CAE),[8] a pediatric epilepsy that is characterized by brief losses of awareness in otherwise normally developing school-aged children. The combined information of DTI and MWI might prove useful in characterizing such subtler changes in myelin content to specific white matter tracts, which may exhibit different development trajectories.

In the current prospective cross-sectional study, we first set out to characterize the maturation of the tract-specific myelin content in healthy subjects from childhood through adolescence into adulthood and subsequently construct a normative graph of white matter tract myelination. Second, we investigate whether tracts that show different maturation trajectories in healthy controls during adolescence (ie, early and late developing tracts) show abnormalities in myelin content in children with CAE compared to healthy controls.

Methods

Participants

Fifteen healthy children (aged 7-12 years), all following regular school without major problems and 14 healthy adult participants (aged 18-32 years) were included in a prospective cross-sectional study. Additionally, seventeen children with a clinical diagnosis of CAE (aged 6-12 years) were included, the inclusion criteria were reported previously.[8] Inclusion of healthy children and children with CAE and adults was approved by the medical ethics committee. All caregivers and participants aged ≥12 years old gave written permission prior to inclusion in the study.

The acquired MR images were visually inspected for motion artifacts. In total, five children (1 healthy control and 4 with CAE) and none of the adults had severe motion artifacts and were removed from subsequent analysis. After exclusion, 14 healthy adults, 14 healthy children, and 13 children with CAE remained for subsequent analysis. The subject characteristics are shown in Table 1. The healthy children and children with CAE did not differ in age and sex.

Table 1. Subject Characteristics

		Children		
	Adults	**Controls**	**CAE**	***P*-value**
Number of subjects	14	14	13	-
Age (years)	28 ± 3.4	9.8 ± 1.9	9.0 ± 2.0	.26
Sex (M/F)	8/6	11/3	9/4	.58
Age of onset (years)	-	-	7.9 ± 2.0	

Data represent mean ± standard deviation unless otherwise indicated. Note that the p-value indicates differences between children with CAE and healthy children. CAE, childhood absence epilepsy; M, male; F, female.

MRI Acquisition

All participants were scanned on a 3 Tesla MRI unit (Philips Achieva, Best, the Netherland) using a 32-element phased array coil.

CAE and Healthy Children Dataset

First, for anatomical reference and segmentation, T1-weighted 3D fast gradient echo images were acquired (repetition time (TR) = 8.36 ms, echo time (TE) = 3.84 ms, flip angle (FA) = 8°, cubic voxel size = 1 mm). For MWF estimation, whole cerebrum 2D multi-slice gradient and spin echo (GRASE) images were acquired (TR = 3000 ms, 32 echoes with 9.3 ms echo spacing, range 9.3-297.6 ms, EPI factor = 3, Turbo factor = 32, 24 slices, 1 mm slice gap, field of view = 228 × 180 × 119 mm, acquisition matrix 152 × 120, voxel size = 1.5 × 1.5 × 4 mm) with parallel acquisition (sensitivity encoding, SENSE = 2) and a scan duration of 5:45 minutes. To reconstruct the tracts in the white matter, diffusion weighted images were acquired (TR = 6579 ms, TE = 74 ms, cubic voxel size = 2 mm, b value 1200 s/mm^2, 66 gradient directions and a single non-diffusion weighted b = 0 image, acquisition time 7:34 min).

Adult Dataset

First, for anatomical reference and segmentation, T1-weighted 3D fast gradient echo images were acquired (repetition time (TR) = 8.14 ms, echo time (TE) = 3.73 ms, flip angle (FA) = 8°, cubic voxel size = 1 mm). For MWF estimation, whole cerebrum 2D multi-slice gradient and spin echo (GRASE) images were acquired (TR = 3000 ms, 32 echoes with 10 ms echo spacing, range 10–320 ms, EPI factor = 3, Turbo factor = 32, 26 slices, 1 mm slice gap, field of view = 240 × 198 × 130 mm, acquisition matrix 160 × 132, voxel size = 1.5 × 1.5 × 4 mm) with parallel acquisition (sensitivity encoding, SENSE = 2), and a scan duration of 7:34 minutes. To estimate the reproducibility of tract-specific MWF estimation, a second GRASE scan was acquired for six volunteers.[20] To calculate the tract tracts in the white matter, diffusion weighted images were acquired (TR = 7012 ms, TE = 74 ms, cubic voxel size = 2 mm, b value = 1200 s/mm^2, 66 gradient directions, and a single non-diffusion weighted b = 0 image, acquisition time 8:03 min).

Analysis

Anatomical Parcellation

Using Freesurfer, 68 cortical regions from the Desikan-Killiany atlas as well as 16 subcortical regions were automatically segmented from the T1-weighted images.[21] Subsequently, the T1-weighted image and resulting atlas were resampled to the voxel size of the DTI images ($2 \times 2 \times 2$ mm).

Myelin-Water Fraction Calculation

To reduce noise in the multi-echo data, a singular value decomposition (SVD) filter was used,[22] as well as a Gaussian filter with a kernel size of 5×5 and FWHM of 1.1 mm to spatially smooth the images. Multi-exponential analysis of the multi-echo data was performed using the non-negative least squares (NNLS) algorithm.[23] Using a basis set of 120 logarithmically spaced relaxation functions (T2 range 15-2000 ms) the NNLS estimates the contribution of each relaxation function to the measured multi-echo data. The algorithm was regularized using an additional minimal energy constraint that allows an increased misfit between 2% and 2.5% ($1.020 \leq \chi_{reg}/\chi_{min} \leq 1.025$).[24] To model the decay more accurately, both B1 inhomogeneities and imperfect slice profiles were considered, as has been described previously.[20] Subsequently, the MWF was calculated as the ratio of myelin-water associated T2 components (15-40 ms) to all T2 components (15-2000 ms). The MWF maps were co-registered and resliced to the resampled T1-weighted images in MATLAB R2016b using the statistical parametric mapping (SPM12, https://www.fil.ion.ucl.ac.uk/spm/software/spm12/) toolkit.[25]

Tract Tractography

The preprocessing and tract tracking of the DTI data were performed using ExploreDTI v4.8.6.[26] The diffusion MRI data was first corrected for head displacement, including B-matrix rotation, and Eddy current induced geometric distortions. Subsequently, an EPI distortion correction was performed by transforming the diffusion images to the resampled T1-weighted space. Whole brain tract tractography was performed using constrained spherical deconvolution with a uniform seed point of 2 mm^3, a step size of 1 mm, angle threshold 30° and tract length range 50-500 mm.

Structural Network Construction

To construct the structural brain network, we used the 84 Freesurfer brain regions as nodes. Subsequently, using ExploreDTI, the number of streamlines (ie, tracts) between each pair of nodes was calculated. To minimize the number of unstable and spurious connections, two nodes were considered connected if there are at least two streamlines between them.[27] Furthermore, we impose that the total tract volume is at least 400 mm^3 (=50 voxels). The latter requirement was added since the myelin maps have thicker slices (4 mm) compared to the diffusion images (2 mm), potentially causing unreliable results for tracts with a small volume. Moreover, only the tracts with a fair or better reproducibility of MWF values were included. Therefore, the intra-class correlation coefficient (ICC) was calculated for each tract using a one-way random model, and only those tracts with ICC > .40 were selected for further analysis.[28] Finally, to avoid results based on a small number of data points, only edges present in at least 50% of the adults, 50% of the healthy children and 50% of the children with CAE were considered (ie, group-thresholding).[29]

To evaluate the robustness of our results, we have also constructed the structural graph while varying the aforementioned tuning parameters (3 and 5 streamlines between nodes, imposing a tract volume of 80 mm^3 (=10 voxels) and 800 mm^3 (=100 voxels), without the ICC constraint and with group-thresholds of 25% and 75%).

To construct the MWF weighted network, the median MWF was calculated for each of the tracts connecting nodes, by extracting the tract mask using ExploreDTI and overlaying it on the MWF map. The median, instead of the mean, was used, since the MWF distribution in a region of interest is skewed.[20,30,31]

Maturation Analysis

The effect of age on the tract-specific myelin content was derived from the healthy subjects using linear regression. Previous studies suggest a nonlinear, reversed U-shaped, relation between myelin content and age,[12,32,33] therefore a quadratic age term was added to the model.

Using the regression formula, the tract-specific myelin-water content was calculated for the representative ages of 12 (MWF_{12y}) and 25 (MWF_{25y}) years. Subsequently, the percentual difference in myelin-water content (PDMW) at 25 years compared to 12 years was calculated as:

$$PDMW = \frac{MWF_{25y} - MWF_{12y}}{MWF_{12y}} \times 100\%$$

Note that the PDMW can also yield negative values, indicating a decrease in myelin-water content.

A tract-specific myelin developmental graph was obtained by calculating the PDMW for each tract. The graph can be used to differentiate tracts based on their myelin development.

To investigate developmental differences between healthy children and children with CAE, two types of tracts were considered. The tracts that show the least myelin increase (the 10% tracts with the lowest PDMW) and the tracts with a high increase of myelin content (the 10% tracts with the highest PDMW).

To evaluate the development of the non-myelin specific DTI metrics (FA and RD), we also used the FA and RD to construct developmental graphs based on their respective percentual differences (PDFA and PDRD).

Statistical Analysis

Differences in PDMW values in the healthy controls were examined between the tracts only traversing inside the left and right hemispheres (ie, intra-hemispheric tracts) using an independent samples *t*-test. Using a similar approach, differences between intra- and interhemispheric, anterior (frontal lobe) and posterior (occipital and parietal lobes) as well as central (subcortical, cingulate, and insular regions) and peripheral connections were assessed.

Differences in myelin-water content of early and late developing tracts between the healthy children and children with CAE were estimated using multivariate regression analysis. Age and sex were added to the model as covariates. To evaluate the robustness of the results, the analysis was repeated for 25% and 50% of the tracts (instead of 10%) with the lowest/highest PDMW values.

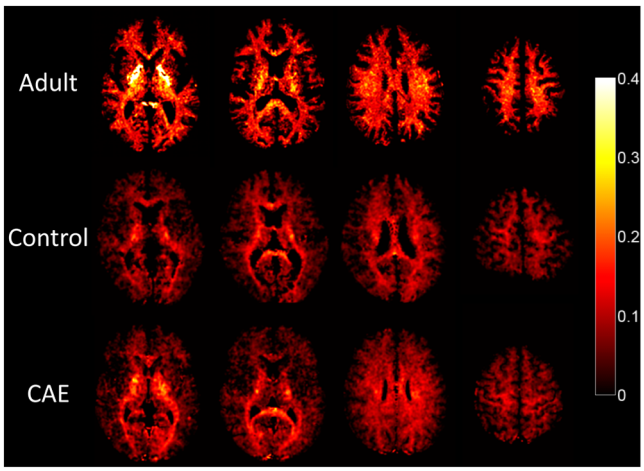

Fig. 1. Example MWF maps of an adult (28 year old male), healthy control child (9 year old boy) and child with childhood absence epilepsy (10 year old boy).

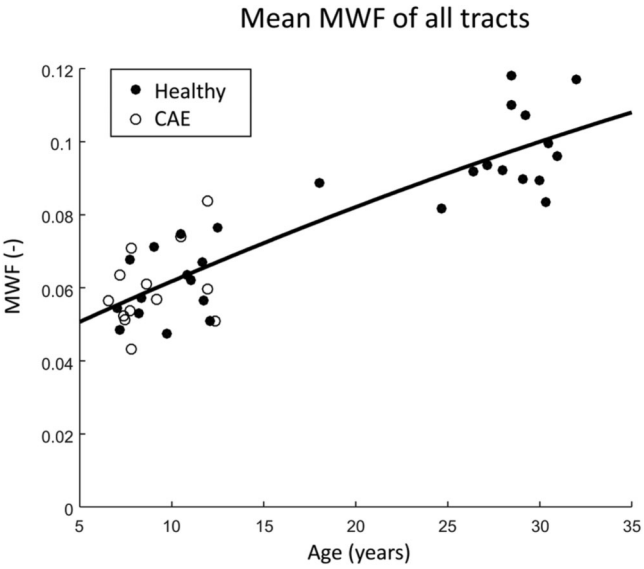

Fig. 2. Mean MWF of all tracts of healthy subjects and children with CAE with respect to age. The solid curve represents a quadratic least-squares fit. Abbreviations: MWF, myelin-water fraction; CAE, childhood absence epilepsy.

Statistical analysis was performed using MATLAB R2016, and statistical significance was inferred when $P < .05$.

Results

Resulting MWF maps are shown in Figure 1, for a representative healthy adult, healthy child, and child with CAE. In Figure 2 the mean MWF of all the tracts is shown as a function of age. The solid curve represents a least squares quadratic fit ($R^2 = .77$, $P < .01$). The mean MWF for the healthy children ($.060 \pm .011$) and children with CAE ($.060 \pm .011$) is similar, while the healthy adults have a higher mean MWF ($.097 \pm .012$).

The tract-specific PDMW graph from childhood (12 years) to adulthood (25 years) is shown in Figure 3A, a histogram with the PDMW values is shown in Figure 3B. Figure 3C shows the 10% tracts with the lowest MWF increase, and Figure 3D, the 10% tracts with the highest MWF increase. The resulting PDMW graph is publicly available on GitHub (https://github.com/GSDrenthen/MWFDevelopmantGraph). Table 2 shows the PDMW for several groups of tracts. The PDMW values of the tracts in the right hemisphere, intra-hemispheric tracts, and peripheral tracts are significantly higher compared to tracts in the left hemisphere, inter-hemispheric tracts, and central tracts, respectively. PDMW values of anterior tracts did not differ significantly from posterior tracts.

No significant differences were found in MWF content between healthy children and children with CAE for either the tracts that develop in an early stage ($\beta = -.15$, $P = .49$) (Fig 3C), or the tracts that develop in a later stage ($\beta = .26$, $P = .20$) (Fig 3D). However, the difference between the MWF of late and early developing tracts is significantly smaller in the children with CAE ($\beta = -.58$, $P < .01$) (Fig 4). Note that the selection of early and late developing tracts was based on healthy controls only.

When selecting 25% or 50% of the tracts (instead of 10%) with the highest and lowest PDMW values the results are similar, showing that the difference between the MWF of late and early developing tracts (Δ) is significantly smaller in the children with CAE ($P < .01$). Furthermore, varying the tuning parameters of the structural network construction also revealed similar results, showing similar developmental patterns (data not shown) and showing that the Δ is significantly smaller in the children with CAE ($P < .05$).

The PDFA values ($2 \pm 7\%$) and PDRD values ($-2 \pm 5\%$) are much lower compared to the PDMW ($40 \pm 14\%$). Moreover, the developmental patterns were less pronounced compared to the PDMW graph (data not shown). Furthermore, while for the PDRD graph the Δ is still significantly different in children with CAE ($P < .05$), no significant difference was reported for the Δ in the PDFA graph.

Discussion

Current Findings

This study characterized a whole brain tract-specific myelin development graph for children aged from 7 to 12 years and adults aged from 18 to 32 years, and assessed differences of tract-specific myelin-water content in children with CAE. Tract-specific myelin-water content is shown to develop through adulthood. Especially, the tracts connecting central regions, inter-hemispheric connections, and tracts in the left hemisphere are shown to be myelinated in an earlier stage compared to the peripheral regions, intra-hemisphere, and right hemisphere connections, respectively. Furthermore, cross-sectional differences in myelin-water content of early and late developing tracts (as determined in healthy controls) were found between children with CAE and healthy controls.

Maturation of Myelin Content

Myelination proceeds rapidly after birth and during infancy and early childhood.[5,16] Here, the myelin content is shown to increase from childhood through adolescence into adulthood, as was also reported previously.[32,34] Interestingly, the diffusion metrics FA and RD showed much less pronounced increases, indicating that although they are sensitive to the myelin content, they fail to be specific to the myelin content only. By determining the development of tract-specific myelin content,

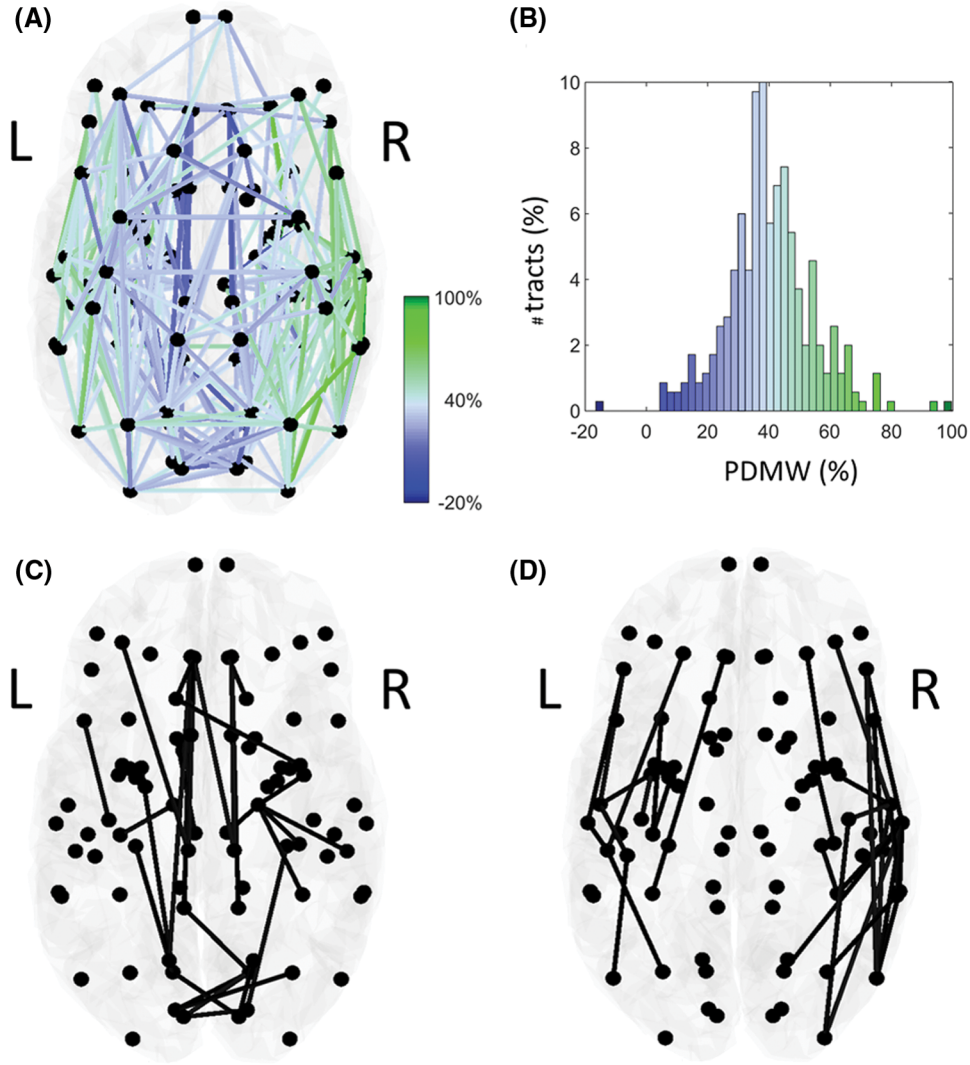

Fig. 3. (A) Myelin development graph, showing the tract-specific PDMW values, (B) histogram of the PDMW values, (C) the 10% tracts with the lowest percentual MWF increase, and (D) the 10% with the highest percentual MWF increase. Abbreviations: L, left; R, right; MWF, myelin-water fraction; PDMW, percentual difference in myelin-water content.

different development trajectories can be observed for different tract bundles. Early myelination is considered to develop from inward to outward regions and from posterior to anterior regions,[35] which is partly in agreement to our current findings. While the tracts connecting central structures (sub-cortical, cingulate, and insular) are developed in an earlier stage compared to outward regions, no difference was found between tracts in posterior and anterior regions. This possibly indicates that the posterior-anterior development of myelin content precedes largely the age of 12 years, while the inward-outward pattern persists into adulthood.

The tracts in the left hemisphere had lower PDMW values compared to the right hemisphere, indicating that the tracts in the left hemisphere are myelinated in an earlier stage. In most individuals, language processes are strongly left-lateralized.[36,37] Similar leftward asymmetries in myelin-water content were previously related to language ability in young children (aged 1-5 years).[38] Although language development peaks at these early ages, it continues through adolescence into adulthood.[39] Therefore, the persisting asymmetry that we observed between 12 and 25 years of age is likely to be related to language development.

Table 2. PDMW Values for Several Tract Types in Healthy Controls

Tract types	PDMW	*P*-value
Left hemisphere	40 ± 13%	<.01
Right hemisphere	45 ± 16%	
Intra-hemisphere	42 ± 14%	<.01
Inter-hemisphere	35 ± 10%	
Anterior	34 ± 9%	.13
Posterior	36 ± 12%	
Central	19 ± 17%	<.01
Peripheral	43 ± 14%	

Data represent mean ± standard deviation unless otherwise indicated. PDMW, percentual differences in myelin-water content.

Myelin Abnormalities in CAE

Children with CAE showed cross-sectional differences in myelin-water content of tracts with different maturation trajectories, as determined in healthy controls. Namely, children with CAE showed a lower difference in myelin-water content between the earlier and later developing tracts. This finding may exhibit the effect that epilepsy has on the development of

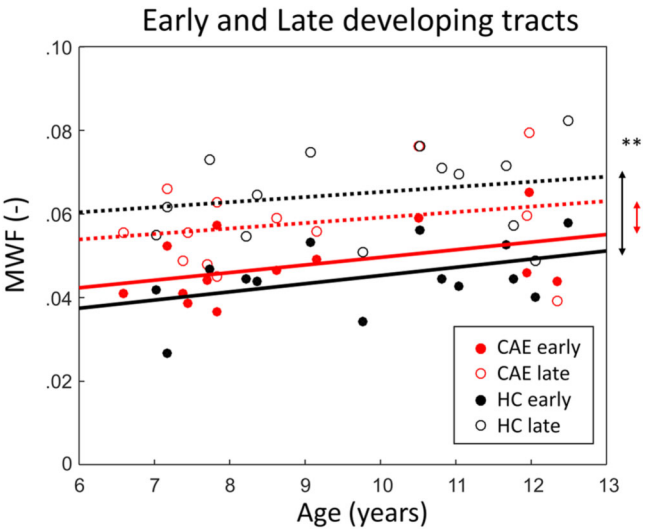

Fig. 4. Myelin-water content of early (solid lines and closed circles) and late developing tracts (dashed lines and open circles) in children with childhood absence epilepsy (CAE; red) and healthy peers (HC; black). The difference between the myelin-water fraction (MWF) of late and early developing tracts is significantly smaller in children with CAE (red arrow) compared to controls (black arrow). $^{**}P < .01$.

various white matter tracts during childhood. The widespread myelin developmental differences might play a role in the underlying mechanisms of CAE. The main function of myelin is accelerating the propagation velocity of electrical signals via saltatory conduction. Differences in myelin content could impact the complex temporal organization of action potentials,[40] and therefore might play a role in the synchronized neuronal activity during generalized seizures that accompany CAE. A previous study with the same cohort already showed a decreased myelin-water content in the frontal lobe of children with CAE.[8] Thus, besides a lobular decrease of frontal myelin content shown earlier, this study shows a more widespread difference in neurodevelopment as part of CAE.

Study Considerations

Our study has important strengths. The study used well defined inclusion criteria for children with CAE in agreement with current ILAE standards. Moreover, the age and sex-matched controls enabled us to make reliable group-level comparisons. This study has two major limitations. The first limitation of the study is the different acquisition resolution of the diffusion and GRASE images, resulting in additional preprocessing steps (interpolation, co-registration) that could introduce artifacts in the results. Accordingly, only tracts of sufficient volume (50 voxels) and reproducible MWF values were included in the analysis. Second, the acquisition parameters of the MRI exams differ slightly between the children and adults. The TR of the diffusion weighted scan is 7012 ms in the adult dataset and 6579 ms in the children dataset while the TE spacing for the GRASE scan is 9.3 ms in the children and 10 ms in the adults. It cannot be fully excluded that these differences may have a bearing on our results, though in-house simulations revealed that the MWF values of the two scans are closely related to a linear model with unit slope and zero intercept ($R^2 > .95$). Moreover, for the group-comparison, the myelin-water content in CAE was compared to healthy control scans with the same acquisition parameters. Additionally, diffusion MRI acquisition is prone to EPI distortions, especially the frontal and temporal lobe are susceptible to such artifacts. While an EPI correction was performed, it cannot be excluded that some regions are still affected by EPI distortions. Furthermore, healthy development of myelin-content between the ages of 12 and 25 was assessed cross-sectionally. While our results indicate that the patterns of maturation presented are in agreement with most evidence from other studies, a more accurate overview of maturation effects should be made with longitudinal data. Similarly, the neurodevelopmental difference in CAE is based on the maturation graph from healthy controls. Moreover, the sample size of this study is relatively small, which limits the power for more in-depth correlation analysis with clinical/epilepsy variables. Future larger studies with longitudinal data, or even adults who were previously diagnosed with CAE, could provide additional insights into the neurodevelopmental involvement of myelin content in CAE.

Concluding Remark

This study investigated the development of healthy tract-specific myelin-water content. Myelin content was found to increase steadily throughout the whole brain from childhood into adulthood. Clear patterns of maturation were observed, where tracts in the central regions myelinate prior to peripheral tracts and intra-hemispheric tracts as well as tracts in the left hemisphere myelinate prior to inter-hemispheric tracts and tracts in the right hemisphere, respectively. The latter possibly due to language development. The development graph was applied to a cohort of children with CAE and healthy controls. The difference between earlier and later myelinated tracts was lower in children with CAE, indicating that CAE is associated with widespread neurodevelopmental myelin differences.

References

1. Baraban M, Mensch S, Lyons DA. Adaptive myelination from fish to man. Brain Res 2016;1641:149-61.
2. Morris SR, Holmes RD, Dvorak AV, et al. Brain myelin water fraction and diffusion tensor imaging atlases for 9-10 year-old children. J. Neuroimaging 2020;30:150-60.
3. Valk J, van der Knaap MS. Myelination and retarded myelination. In: *Magnetic Resonance of Myelin, Myelination, and Myelin Disorders.* Berlin, Heidelberg: Springer, 1989:26-65.
4. Williamson JM, Lyons DA. Myelin dynamics throughout life: an ever-changing landscape? Front Cell Neurosci 2018;12:424.
5. Carmody DP, Dunn SM, Boddie-willis AS. A quantitative measure of myelination development in infants, using MR images. Neuroradiology 2004;46:781-6.
6. Kavroulakis E, Simos PG, Kalaitzakis G, et al. Myelin content changes in probable Alzheimer's disease and mild cognitive impairment: associations with age and severity of neuropsychiatric impairment. J Magn Reson Imaging 2018;47:1359-72.
7. Kolind S, Seddigh A, Combes A, et al. Clinical brain and cord myelin water imaging: a progressive multiple sclerosis biomarker. Neuroimage Clin 2015;9:574-80.
8. Drenthen GS, Fonseca Wald ELA, Backes WH, et al. Lower myelin-water content of the frontal lobe in childhood absence epilepsy. Epilepsia 2019;60:1689-96.
9. Dean DC III, Sojkova J, Hurley S, et al. Alterations of myelin content in parkinson's disease: a cross-sectional neuroimaging study. PLoS One 2016;11:e0163774.
10. Lang DJM, Yip E, Mackay AL, et al. Clinical 48 echo T2 myelin imaging of white matter in first-episode schizophrenia: Evidence for aberrant myelination. NeuroImage Clin 2014;6:408-14.

11. Bouhrara M, Reiter DA, Bergeron CM, et al. Evidence of demyelination in mild cognitive impairment and dementia using a direct and specific magnetic resonance imaging measure of myelin content. Alzheimers Dement 2018;14:998-1004.
12. Lebel C, Treit S, Beaulieu C. A review of diffusion MRI of typical white matter development from early childhood to young adulthood. NMR Biomed 2019;32:e3778.
13. Laule C, Vavasour IM, Kolind SH, et al. Magnetic resonance imaging of myelin. Neurotherapeutics 2007;4:460-84.
14. Kumar R, Nguyen HD, Macey PM, et al. Regional brain axial and radial diffusivity changes during development. J Neurosci Res 2012;90:346-55.
15. Janve VA, Zu Z, Yao SY, et al. The radial diffusivity and magnetization transfer pool size ratio are sensitive markers for demyelination in a rat model of type III multiple sclerosis (MS) lesions. Neuroimage 2013;74:298-305.
16. Mackay AL, Laule C. Magnetic Resonance of myelin water: an in vivo marker for myelin. Brain Plast 2016;2:71-91.
17. Alonso-Ortiz E, Levesque IR, Pike GB. MRI-based myelin water imaging: a technical review. Magn Reson Med 2015;73:70-81.
18. Baumeister TR, Kolind SH, MacKay AL, et al. Inherent spatial structure in myelin water fraction maps. Magn Reson Imaging 2019;67:33-42.
19. Mancini M, Giulietti G, Dowell N, et al. Introducing axonal myelination in connectomics: A preliminary analysis of g-ratio distribution in healthy subjects. Neuroimage 2017;182:351-9.
20. Drenthen GS, Backes WH, Aldenkamp AP, et al. Applicability and reproducibility of 2D multi-slice GRASE myelin water fraction with varying acquisition acceleration. Neuroimage 2019;195: 333-9.
21. Desikan RS, Ségonne F, Fischl B, et al. An automated labeling system for subdividing the human cerebral cortex on MRI scans into gyral based regions of interest. Neuroimage 2006;31:968-80.
22. Bydder M, Du J. Noise reduction in multiple-echo data sets using singular value decomposition. Magn Reson Imaging 2006;24:849-56.
23. Whittall KP, MacKay AL. Quantitative interpretation of NMR relaxation data. J Magn Reson 1989;84:134-52.
24. Skinner MG, Kolind SH, MacKay AL. The effect of varying echo spacing within a multiecho acquisition: better characterization of long T2 components. Magn Reson Imaging 2007;25:840-7.
25. Friston KJ, Ashburner J, Kiebel S, et al., eds. *Statistical Parametric Mapping*. Amsterdam: Elsevier; 2007.
26. Leemans A, Jeurissen B, Sijbers J, et al. ExploreDTI: a graphical toolbox for processing, analyzing, and visualizing diffusion MR data. Proc 17th Sci Meet Int Soc Magn Reson Med 2009;17:3537.
27. Ma J, Kang HJ, Kim JY, et al. Network attributes underlying intellectual giftedness in the developing brain. Sci Rep 2017;1-9.
28. Cicchetti DV. Guidelines, criteria, and rules of thumb for evaluating normed and standardized assessment instruments in psychology. Psychol Assess 1994;6:284-90.
29. De Reus MA, Van Den Heuvel MP. Estimating false positives and negatives in brain networks. Neuroimage 2013;70:402-9.
30. Kolind S, Matthews L, Johansen-berg H, et al. Myelin water imaging reflects clinical variability in multiple sclerosis. Neuroimage 2012;60:263-70.
31. Dayan M, Hurtado Rúa SM, Monohan E, et al. MRI analysis of white matter myelin water content in multiple sclerosis: a novel approach applied to finding correlates of cortical thinning. Front Neurosci 2017;11:284.
32. Arshad M, Stanley JA, Raz N. Adult age differences in subcortical myelin content are consistent with protracted myelination and unrelated to diffusion tensor imaging indices. Neuroimage 2016;143:26-39.
33. Bouhrara M, Rejimon AC, Cortina LE, et al. Neurobiology of aging adult brain aging investigated using BMC-mcDESPOT e based myelin water fraction imaging. Neurobiol Aging 2020;85:131-9.
34. Geeraert BL, Lebel RM, Lebel C. A multiparametric analysis of white matter maturation during late childhood and adolescence. Hum Brain Mapp 2019;40:4345-56.
35. Dietrich R, Bradley W, Zaragoza 4th E, et al. MR evaluation of early myelination patterns in normal and developmentally delayed infants. Am J Roentgenol 1988;150:889-96.
36. Ocklenburg S, Friedrich P, Fraenz C, et al. Neurite architecture of the planum temporale predicts neurophysiological processing of auditory speech. Sci Adv 2018;4:eaar6830.
37. Hugdahl K. Lateralization of cognitive processes in the brain. Acta Psychol 2000;105:211-35.
38. O'Muircheartaigh J, Dean DC, Dirks H, et al. Interactions between white matter asymmetry and language during neurodevelopment. J Neurosci 2013;33:16170-7.
39. Nippold MA. Language development during the adolescent years: aspects of pragmatics, syntax, and semantics. Top Lang Disord 2000;20:15–28.
40. Pajevic S, Basser PJ, Fields RD. Role of myelin plasticity in oscillations and synchrony of neuronal activity. Neuroscience 2014;276:135-47.